
 PHYSICAL CHEMISTRY
 OF SOLUTIONS

Phase and Physicochemical Properties Diagrams of Quaternary System $\text{Li}_2\text{B}_4\text{O}_7 + \text{Na}_2\text{B}_4\text{O}_7 + \text{Mg}_2\text{B}_6\text{O}_{11} + \text{H}_2\text{O}^1$

Shi-qiang Wang*, Xue-min Du, Yan Jing, Ya-fei Guo, and Tian-long Deng

Tianjin Key Laboratory of Marine Resources and Chemistry, College of Chemical Engineering and Materials Science, Tianjin University of Science and Technology, Tianjin 300457, P.R. China

*email: wangshiqiang@tust.edu.cn

Received June 29, 2016

Abstract—The phase and physicochemical properties diagrams of the quaternary system ($\text{Li}_2\text{B}_4\text{O}_7 + \text{Na}_2\text{B}_4\text{O}_7 + \text{Mg}_2\text{B}_6\text{O}_{11} + \text{H}_2\text{O}$) at 288.15 K and 0.1 MPa were constructed using the solubilities, densities, and refractive indices measured. In the phase diagrams of the system there are one invariant point, three univariant isothermic dissolution curves, and three crystallization regions corresponding to $\text{Li}_2\text{B}_4\text{O}_7 \cdot 3\text{H}_2\text{O}$, $\text{Na}_2\text{B}_4\text{O}_7 \cdot 10\text{H}_2\text{O}$, and $\text{Mg}_2\text{B}_6\text{O}_{11} \cdot 15\text{H}_2\text{O}$, respectively. The solution density, refractive index of the quaternary system changes regularly with the increasing of $\text{Li}_2\text{B}_4\text{O}_7$ concentration. The calculated values of density and refractive index using empirical equations of the quaternary system are in good agreement with the experimental values.

Keywords: stable phase equilibrium, phase diagram, lithium borate, borax, inderite

DOI: 10.1134/S0036024417130180

INTRODUCTION

There are more than seven hundred salt lakes with an area larger than 1 km² in the Qinghai-Tibet Plateau. The Salt Lake of Qaidam Basin consists of a series of lakes including the Dong-Xi-Taijinaier lake, Da-Xiao-Chaidan lake, and Yiliping lake, and is one of the subtypes of magnesium sulfate brines famous for its abundance of lithium, potassium, and boron resources [1–4]. The main components of its brines can be described with the $\text{Li}^+ + \text{Na}^+ + \text{K}^+ + \text{Mg}^{2+} + \text{Cl}^- + \text{SO}_4^{2-} + \text{borate} + \text{H}_2\text{O}$ system. It is well-known that phase diagrams and phase equilibria play an important role in exploiting brine resources and describing the geochemical behavior of brine mineral. To exploit the valuable brine resources economically, the phase equilibria and phase diagrams of brine systems containing boron at different temperatures are required.

Aiming at understanding the thermodynamic properties of boron-containing brine, some solid-liquid phase equilibria systems at different temperatures have been done by our research group [5–10]. However, the investigations on thermodynamic properties of the aqueous solutions containing borates are lack, this might be due to the variety of the present forms of polyborates, such as diborate ($\text{B}_2\text{O}_4^{2-}$), metaborate (BO_2^-), triborate (B_3O_5^-), and polytetraborate ($\text{B}_4\text{O}_7^{2-}$,

B_5O_8^- , $\text{B}_6\text{O}_{10}^{2-}$), and the dissolving behavior of boron is very complicated. In this paper, the isothermal solubilities and solution density, refractive index of the quaternary system ($\text{Li}_2\text{B}_4\text{O}_7 + \text{Na}_2\text{B}_4\text{O}_7 + \text{Mg}_2\text{B}_6\text{O}_{11} + \text{H}_2\text{O}$) at 288.15 K were presented by the isothermal dissolution equilibrium method to describe the stable behaviors to separate and purify the borate-containing mixture salts.

EXPERIMENTAL

Apparatus and Reagents

A thermostatic water bath (HXC-500-6A, Beijing Fortunejoy Sci. Technol. Co. Ltd.) with magnetic stirring was used to control the temperature with a precision of 0.01 K. Polarized light microscopy (BX51, Olympus Co., Japan) and X-ray powder diffraction (MSAL XD-3, Beijing Purkinje Instrument Co. Ltd., China) were used to identify the solid phases. An inductively coupled plasma optical emission spectrometer (ICP-OES, Prodigy, Leman Co., USA) was employed to determine the concentrations of Li^+ in solutions.

The chemicals of analytical grade were obtained from either Sinopharm Chemical Reagent Co., Ltd.: lithium borate trihydrate ($\text{Li}_2\text{B}_4\text{O}_7 \cdot 3\text{H}_2\text{O}$, 0.992 in mass fraction), borax ($\text{Na}_2\text{B}_4\text{O}_7 \cdot 10\text{H}_2\text{O}$, 0.995 in mass fraction), and were recrystallized with doubly deionized water (DDW) before use. Inderite

¹ The article is published in the original.

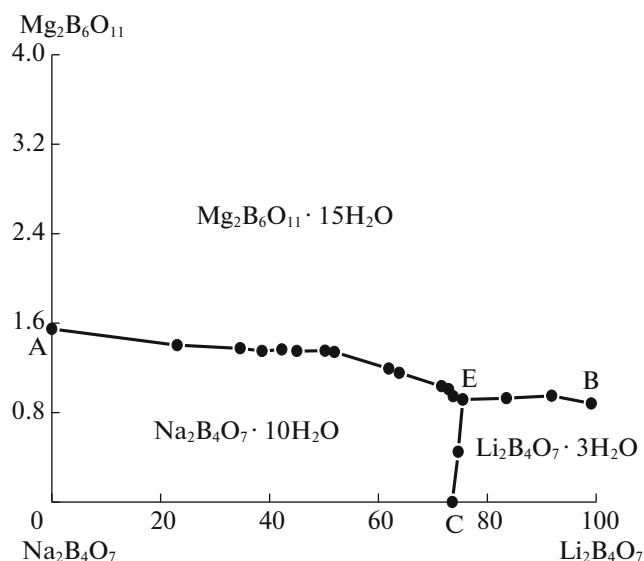


Fig. 1. Dry-salt phase diagram of the quaternary system ($\text{Li}_2\text{B}_4\text{O}_7 + \text{Na}_2\text{B}_4\text{O}_7 + \text{Mg}_2\text{B}_6\text{O}_{11} + \text{H}_2\text{O}$) at 288.15 K.

($\text{Mg}_2\text{B}_6\text{O}_{11} \cdot 15\text{H}_2\text{O}$, 0.99 in mass fraction) was synthesized in our laboratory by the method described in [11]. Doubly deionized water (DDW) with conductivity less than $1 \times 10^{-4} \text{ S m}^{-1}$ was used to prepare the series of the artificial brines and for chemical analysis.

Method

The isothermal dissolution method was used in this study; more details of the experimental method are available in our previous works [12–14]. The series of artificial synthesized complexes are sealed in hard polyethylene bottles and placed in the magnetically stirred thermostatic bath (HXC-500-6A). The temperatures of the baths were set at $288 \pm 0.01 \text{ K}$ with 150 rpm stirring speed in order to accelerate the establishment of equilibrium. After stirring for about 3 to 5 days, it could be found that the equilibrium had been reached when the compositions of the liquid phase became constant. Before sampling, it took about 1 h for the clarification of an aqueous solution. Two samples were taken out from the bottles. One was used for determining physicochemical properties including density and refractive index of the liquid phase. The other is subjected to quantitative analysis. In addition, the solid phases were identified by X-ray powder diffraction.

The concentration of boron in liquid phase was analyzed by the weight methods using mannitol and sodium hydroxide standard solution in the presence of double indicator of methyl red and phenolphthalein, and the relative error of the analytical results is less than ± 0.003 in mass fraction. The Mg^{2+} ion concentration was determined with modified EDTA complexometric titration method in the presence of Erio-

chrome Black T as an indicator. The interference of the lithium ion in brine can be efficiently eliminated using butanol and anhydrous alcohol as a masking agent, and the uncertainty is less than ± 0.003 in mass fraction [15]. The Li^+ concentration was evaluated with ICP-OES measurement.

The measurements of the liquid-phase physicochemical properties were corresponding to density and refractive index. The densities (ρ) were measured using a digital vibrating-tube densimeter (DMA 4500, Anton Paar Co. Ltd., Austria) with an uncertainty of $\pm 0.00001 \text{ g cm}^{-3}$. An Abbe refractometer (WZS-1, Shanghai Yuguang Instrument Co. Ltd., China) was used to measure the refractive index (n_D) with an accuracy of ± 0.0001 . All the measurements were performed at the desired temperature with $\pm 0.01 \text{ K}$ through control of the thermostat (K20-cc-NR, Huber, Germany).

RESULTS AND DISCUSSION

Phase Diagram of the Quaternary System ($\text{Li}_2\text{B}_4\text{O}_7 + \text{Na}_2\text{B}_4\text{O}_7 + \text{Mg}_2\text{B}_6\text{O}_{11} + \text{H}_2\text{O}$)

The experimental data on the solubilities and the relevant physicochemical properties including density and refractive index of the quaternary system ($\text{Li}_2\text{B}_4\text{O}_7 + \text{Na}_2\text{B}_4\text{O}_7 + \text{Mg}_2\text{B}_6\text{O}_{11} + \text{H}_2\text{O}$) at 288.15 K were determined and are presented in Table 1. The composition of the liquid phase in the quaternary system was expressed in mass fraction and Jänecke index (J_b , g/100 g dry salt). According to the experimental data in Table 1, the stable phase diagrams of the quaternary system at 288.15 K were plotted, as shown in Figs. 1 and 2.

In Fig. 1, the dry-salt phase diagram consists of three crystallization zones corresponding to lithium borate trihydrate ($\text{Li}_2\text{B}_4\text{O}_7 \cdot 3\text{H}_2\text{O}$), borax ($\text{Na}_2\text{B}_4\text{O}_7 \cdot 10\text{H}_2\text{O}$), and inderite ($\text{Mg}_2\text{B}_6\text{O}_{11} \cdot 15\text{H}_2\text{O}$); one invariant point E, which are saturated with $\text{Li}_2\text{B}_4\text{O}_7 \cdot 3\text{H}_2\text{O} + \text{Na}_2\text{B}_4\text{O}_7 \cdot 10\text{H}_2\text{O} + \text{Mg}_2\text{B}_6\text{O}_{11} \cdot 15\text{H}_2\text{O} + \text{Liquid}$, three univariant isothermal dissolution curves of AE, BE, and CE, indicating the cosaturation of two salts. Due to the high solubilities of lithium borate and borax, there is a strong salting-out effect to magnesium borate.

Figure 2 is the water-phase diagram of the quaternary system at 288.15 K, and it shows that the Jänecke index values of $J(\text{H}_2\text{O})$ gradually change with increasing $J(\text{Li}_2\text{B}_4\text{O}_7)$.

The solid phase minerals were identified with X-ray diffractometry, hydrated salts including $\text{Li}_2\text{B}_4\text{O}_7 \cdot 3\text{H}_2\text{O}$, $\text{Na}_2\text{B}_4\text{O}_7 \cdot 10\text{H}_2\text{O}$, and $\text{Mg}_2\text{B}_6\text{O}_{11} \cdot 15\text{H}_2\text{O}$ are present in the system, and neither double salts nor solid solutions were found. Figure 3 shows the X-ray diffraction patterns of invariant point. The XRD pattern of the invariant point was well matched to standard diffraction patterns of $\text{Li}_2\text{B}_4\text{O}_7 \cdot 3\text{H}_2\text{O}$, $\text{Na}_2\text{B}_4\text{O}_7 \cdot 10\text{H}_2\text{O}$,

Table 1. Solubility and physicochemical properties of the quaternary system ($\text{Li}_2\text{B}_4\text{O}_7 + \text{Na}_2\text{B}_4\text{O}_7 + \text{Mg}_2\text{B}_6\text{O}_{11} + \text{H}_2\text{O}$) at 288.15 K

No.	Composition of liquid phase $w_i \times 10^2$				Jänecke index J_b , g/100 g dry salt			Density ρ , g cm ⁻³	n_D	Solid phase
	$\text{Li}_2\text{B}_4\text{O}_7$	$\text{Na}_2\text{B}_4\text{O}_7$	$\text{Mg}_2\text{B}_6\text{O}_{11}$	H_2O	$\text{Li}_2\text{B}_4\text{O}_7$	$\text{Na}_2\text{B}_4\text{O}_7$	H_2O			
1, A	0.00	1.78	0.028	98.19	0.00	98.45	5430.97	1.01883	1.3369	$\text{Na}_2\text{B}_4\text{O}_7 \cdot 10\text{H}_2\text{O} + \text{Mg}_2\text{B}_6\text{O}_{11} \cdot 15\text{H}_2\text{O}$
2	0.46	1.51	0.028	98.00	23.02	75.58	4905.01	1.01974	1.3378	$\text{Na}_2\text{B}_4\text{O}_7 \cdot 10\text{H}_2\text{O} + \text{Mg}_2\text{B}_6\text{O}_{11} \cdot 15\text{H}_2\text{O}$
3	0.73	1.35	0.029	97.89	34.61	64.01	4641.58	1.02107	1.3380	$\text{Na}_2\text{B}_4\text{O}_7 \cdot 10\text{H}_2\text{O} + \text{Mg}_2\text{B}_6\text{O}_{11} \cdot 15\text{H}_2\text{O}$
4	0.83	1.29	0.029	97.85	38.62	60.03	4553.33	1.02234	1.3385	$\text{Na}_2\text{B}_4\text{O}_7 \cdot 10\text{H}_2\text{O} + \text{Mg}_2\text{B}_6\text{O}_{11} \cdot 15\text{H}_2\text{O}$
5	0.93	1.24	0.030	97.80	42.27	56.36	4445.45	1.02351	1.3389	$\text{Na}_2\text{B}_4\text{O}_7 \cdot 10\text{H}_2\text{O} + \text{Mg}_2\text{B}_6\text{O}_{11} \cdot 15\text{H}_2\text{O}$
6	1.00	1.19	0.030	97.78	45.05	53.60	4404.50	1.02411	1.3390	$\text{Na}_2\text{B}_4\text{O}_7 \cdot 10\text{H}_2\text{O} + \text{Mg}_2\text{B}_6\text{O}_{11} \cdot 15\text{H}_2\text{O}$
7	1.15	1.11	0.031	97.71	50.20	48.45	4264.91	1.02519	1.3391	$\text{Na}_2\text{B}_4\text{O}_7 \cdot 10\text{H}_2\text{O} + \text{Mg}_2\text{B}_6\text{O}_{11} \cdot 15\text{H}_2\text{O}$
8	1.20	1.08	0.031	97.69	51.93	46.73	4227.13	1.02550	1.3392	$\text{Na}_2\text{B}_4\text{O}_7 \cdot 10\text{H}_2\text{O} + \text{Mg}_2\text{B}_6\text{O}_{11} \cdot 15\text{H}_2\text{O}$
9	1.66	0.99	0.032	97.32	64.89	36.91	3628.56	1.02793	1.3399	$\text{Na}_2\text{B}_4\text{O}_7 \cdot 10\text{H}_2\text{O} + \text{Mg}_2\text{B}_6\text{O}_{11} \cdot 15\text{H}_2\text{O}$
10	1.77	0.97	0.032	97.23	63.85	34.99	3507.50	1.02850	1.3400	$\text{Na}_2\text{B}_4\text{O}_7 \cdot 10\text{H}_2\text{O} + \text{Mg}_2\text{B}_6\text{O}_{11} \cdot 15\text{H}_2\text{O}$
11	2.49	0.95	0.036	96.52	71.63	27.33	2776.87	1.03799	1.3416	$\text{Na}_2\text{B}_4\text{O}_7 \cdot 10\text{H}_2\text{O} + \text{Mg}_2\text{B}_6\text{O}_{11} \cdot 15\text{H}_2\text{O}$
12	2.60	0.93	0.036	96.43	72.91	26.08	2704.26	1.03904	1.3417	$\text{Na}_2\text{B}_4\text{O}_7 \cdot 10\text{H}_2\text{O} + \text{Mg}_2\text{B}_6\text{O}_{11} \cdot 15\text{H}_2\text{O}$
13	2.65	0.91	0.034	96.41	73.73	25.32	2682.42	1.03967	1.3418	$\text{Li}_2\text{B}_4\text{O}_7 \cdot 3\text{H}_2\text{O} + \text{Mg}_2\text{B}_6\text{O}_{11} \cdot 15\text{H}_2\text{O}$
14, B	2.81	0.00	0.025	97.17	99.12	0.00	3427.34	1.03278	1.3404	$\text{Li}_2\text{B}_4\text{O}_7 \cdot 3\text{H}_2\text{O} + \text{Mg}_2\text{B}_6\text{O}_{11} \cdot 15\text{H}_2\text{O}$
15	2.80	0.22	0.029	96.95	91.83	7.22	3179.76	1.03415	1.3408	$\text{Li}_2\text{B}_4\text{O}_7 \cdot 3\text{H}_2\text{O} + \text{Mg}_2\text{B}_6\text{O}_{11} \cdot 15\text{H}_2\text{O}$
16	2.79	0.52	0.031	96.66	83.51	15.56	2893.12	1.03694	1.3409	$\text{Li}_2\text{B}_4\text{O}_7 \cdot 3\text{H}_2\text{O} + \text{Mg}_2\text{B}_6\text{O}_{11} \cdot 15\text{H}_2\text{O}$
17, E	2.72	0.85	0.033	96.40	75.49	23.59	2675.46	1.03988	1.3420	$\text{Li}_2\text{B}_4\text{O}_7 \cdot 3\text{H}_2\text{O} + \text{Na}_2\text{B}_4\text{O}_7 \cdot 10\text{H}_2\text{O} + \text{Mg}_2\text{B}_6\text{O}_{11} \cdot 15\text{H}_2\text{O}$
18, C	2.62	0.94	0.00	96.44	73.60	26.40	2708.99	1.03870	1.3419	$\text{Li}_2\text{B}_4\text{O}_7 \cdot 3\text{H}_2\text{O} + \text{Na}_2\text{B}_4\text{O}_7 \cdot 10\text{H}_2\text{O}$
19	2.67	0.89	0.016	96.42	74.66	24.89	2696.42	1.03941	1.3419	$\text{Li}_2\text{B}_4\text{O}_7 \cdot 3\text{H}_2\text{O} + \text{Na}_2\text{B}_4\text{O}_7 \cdot 10\text{H}_2\text{O}$

and $\text{Mg}_2\text{B}_6\text{O}_{11} \cdot 15\text{H}_2\text{O}$ with powder diffraction file (pdf) number 43–1498, 33–1215, 36–0423, respectively. It shows that salts $\text{Li}_2\text{B}_4\text{O}_7 \cdot 3\text{H}_2\text{O}$, $\text{Na}_2\text{B}_4\text{O}_7 \cdot 10\text{H}_2\text{O}$, and $\text{Mg}_2\text{B}_6\text{O}_{11} \cdot 15\text{H}_2\text{O}$ coexist at the invariant point. The compositions of $\text{Li}_2\text{B}_4\text{O}_7$, $\text{Na}_2\text{B}_4\text{O}_7$, $\text{Mg}_2\text{B}_6\text{O}_{11}$ at the invariant point in the liquid phase with mass fraction (10^2w) are 2.72, 0.85, and 0.033, respectively.

The Solution Physicochemical Properties of the Quaternary System

On the basis of experimental data in Table 1, relationship of the solution density and refractive index with the concentration of $\text{Li}_2\text{B}_4\text{O}_7$ in the quaternary system ($\text{Li}_2\text{B}_4\text{O}_7 + \text{Na}_2\text{B}_4\text{O}_7 + \text{Mg}_2\text{B}_6\text{O}_{11} + \text{H}_2\text{O}$) at 288.15 K was plotted in Fig. 4. It was found that the solution density and refractive index in the quaternary system changed regularly with the increasing of $\text{Li}_2\text{B}_4\text{O}_7$ concentration.

In Fig. 4a, the density curves of the equilibrium liquid phase increased gradually with the increasing concentration of $\text{Li}_2\text{B}_4\text{O}_7$ (curves AE and CE), and reached the maximum value of $1.03988 \text{ g cm}^{-3}$ at the

invariant point E, and then the solution densities was decreased sharply with the increasing concentration of $\text{Li}_2\text{B}_4\text{O}_7$ (curve EB).

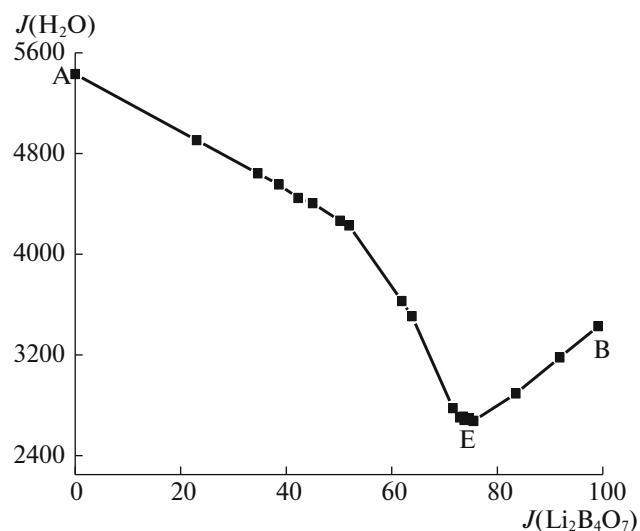


Fig. 2. Water-phase diagram of the quaternary system ($\text{Li}_2\text{B}_4\text{O}_7 + \text{Na}_2\text{B}_4\text{O}_7 + \text{Mg}_2\text{B}_6\text{O}_{11} + \text{H}_2\text{O}$) at 288.15 K.

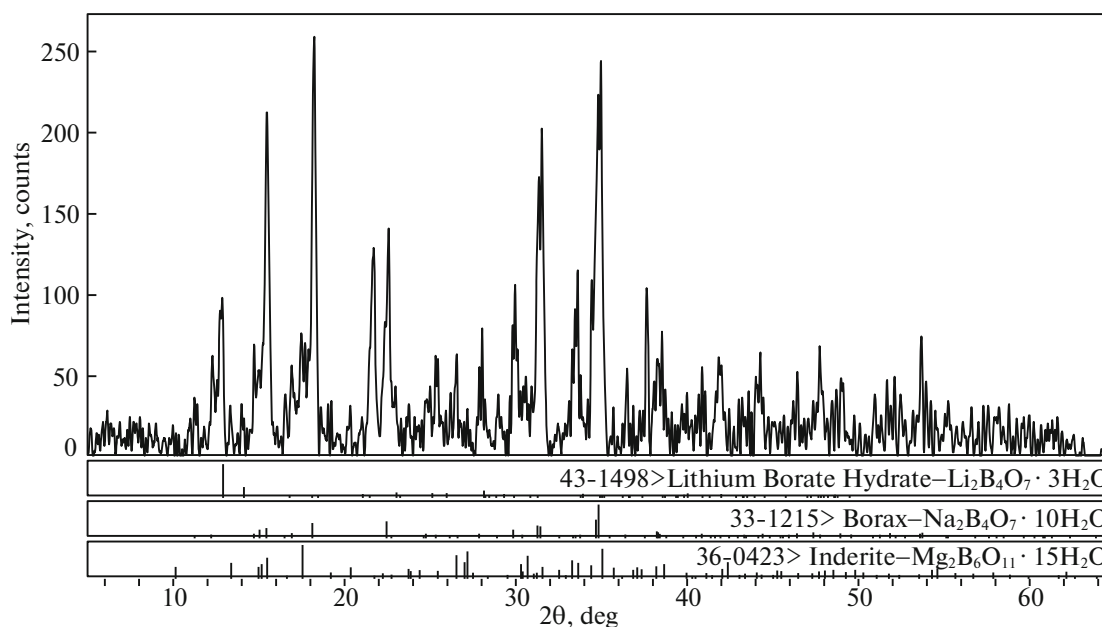


Fig. 3. X-ray diffraction pattern of the invariant point ($\text{Li}_2\text{B}_4\text{O}_7 \cdot 3\text{H}_2\text{O} + \text{Na}_2\text{B}_4\text{O}_7 \cdot 10\text{H}_2\text{O} + \text{Mg}_2\text{B}_6\text{O}_{11} \cdot 15\text{H}_2\text{O}$).

Figure 4b shows the refractive index value versus composition of $\text{Li}_2\text{B}_4\text{O}_7$ in the solution. Similarly as the density in the solution, the refractive index value was increased slowly from point A to point E, while decreased sharply from point E to point B with the increasing concentration of $\text{Li}_2\text{B}_4\text{O}_7$, and the maximum value of 1.3420 at the invariant point E.

Empirical Equations for Density and Refractive Index

Based on the following empirical equations of the density and refractive index in electrolyte solutions developed in the previous study [16], the density and refractive index of the solution were also calculated.

$$\ln \frac{\rho_i}{\rho_0} = \sum A_i w_i, \quad \ln \frac{n_{Di}}{n_{D0}} = \sum B_i w_i. \quad (1)$$

In the above equations, where ρ_i and ρ_0 are the densities of the solution and the pure water at the same temperature; the ρ_0 value of pure water at 288.15 K is $0.99909 \text{ g cm}^{-3}$; while n_{Di} and n_{D0} refer the refractive index value of the solution and the pure water at the same temperature; the n_{D0} value of pure water at 288.15 K is 1.33339 [17]; A_i and B_i are the constants of each possible component i in the system, and they were calculated in the present work; w_i is the salt of i in the solution with weight percentage, in mass fraction. Constants A_i of $\text{Li}_2\text{B}_4\text{O}_7$, $\text{Na}_2\text{B}_4\text{O}_7$, and $\text{Mg}_2\text{B}_6\text{O}_{11}$ for calculation of density in solution are 0.01178, 0.00959, and 0.00961 at 288.15 K, and con-

stants B_i of $\text{Li}_2\text{B}_4\text{O}_7$, $\text{Na}_2\text{B}_4\text{O}_7$, and $\text{Mg}_2\text{B}_6\text{O}_{11}$ for calculation of refractive index in solution are 0.00278, 0.00252, and 0.00233 at 288.15 K, respectively. All calculated results with the maximum relative error are less than 0.25%. The calculated values agree well with the experimental data, and this agreement shows that the coefficients A_i and B_i obtained in this work are reliable and can be used for more complicated systems containing borate.

CONCLUSIONS

The solubility, solution density and refractive index of the quaternary system ($\text{Li}_2\text{B}_4\text{O}_7 + \text{Na}_2\text{B}_4\text{O}_7 + \text{Mg}_2\text{B}_6\text{O}_{11} + \text{H}_2\text{O}$) were determined using the isothermal dissolution method at 288.15 K. According to experimental data, the equilibrium phase diagrams and the diagrams of physicochemical properties versus concentration of $\text{Li}_2\text{B}_4\text{O}_7$ were constructed. Phase diagram of the quaternary system consists of one invariant point ($\text{Li}_2\text{B}_4\text{O}_7 \cdot 3\text{H}_2\text{O} + \text{Na}_2\text{B}_4\text{O}_7 \cdot 10\text{H}_2\text{O} + \text{Mg}_2\text{B}_6\text{O}_{11} \cdot 15\text{H}_2\text{O} + \text{Liquid}$) and three crystallization regions corresponding to $\text{Li}_2\text{B}_4\text{O}_7 \cdot 3\text{H}_2\text{O}$, $\text{Na}_2\text{B}_4\text{O}_7 \cdot 10\text{H}_2\text{O}$, and $\text{Mg}_2\text{B}_6\text{O}_{11} \cdot 15\text{H}_2\text{O}$. The solution density and refractive index in the quaternary system changed regularly with increasing $\text{Li}_2\text{B}_4\text{O}_7$ concentration. The calculated values of density and refractive index using empirical equations for the quaternary system ($\text{Li}_2\text{B}_4\text{O}_7 + \text{Na}_2\text{B}_4\text{O}_7 + \text{Mg}_2\text{B}_6\text{O}_{11} + \text{H}_2\text{O}$) at 288.15 K are in good agreement with the experimental values.

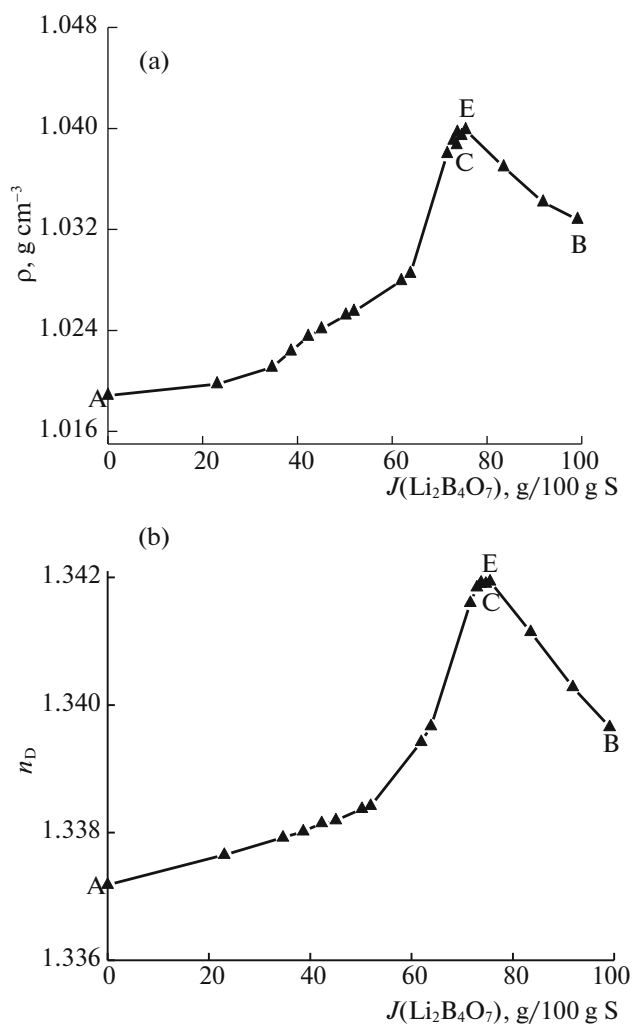


Fig. 4. Physicochemical properties of the solution versus composition diagram of the quaternary system ($\text{Li}_2\text{B}_4\text{O}_7 + \text{Na}_2\text{B}_4\text{O}_7 + \text{Mg}_2\text{B}_6\text{O}_{11} + \text{H}_2\text{O}$) at 288.15 K; (a) density versus composition, (b) refractive index versus composition.

ACKNOWLEDGMENTS

The work was supported by the program of the National Natural Science Foundation of China (nos. U1507109, U1407113, 21406048, 21306136,

21276194, and 21106103), the Program for Changjiang Scholars and Innovative Research Team in University (IRT-17R81), the Innovative Research Team of Tianjin Municipal Education Commission (TD12-5004), and the Natural Science Foundation of Tianjin (no. 17JCYBJC19500), the Specialized Research Fund for Doctoral Program of Chinese Higher Education (no. 20111208120003), and the foundation of Tianjin Key Laboratory of Marine Resources and Chemistry (no. 201401) are greatly acknowledged.

REFERENCES

1. P. S. Song and Y. Yao, *Calphad* **25**, 329 (2001).
2. S. Y. Gao, P. S. Song, S. P. Xia, and M. P. Zheng, *Tibet Saline Lake Chemistry: A New Type of Boron Lithium Salt Lake* (Chin. Sci., Beijing, 2007).
3. X. Y. Zheng, M. G. Zhang, Y. Xu, et al., *Salt Lakes in China* (Chin. Sci., Beijing, 2002).
4. S. Q. Wang and T. L. Deng, *J. Chem. Thermodyn.* **40**, 1007 (2008).
5. D. L. Gao, Q. Wang, Y. F. Guo, et al., *Fluid Phase Equilib.* **371**, 121 (2014).
6. S. Q. Wang, Y. F. Guo, J. S. Yang, et al., *Russ. J. Phys. Chem. A* **89**, 2190 (2015).
7. S. Q. Wang, Y. F. Guo, W. J. Liu, et al., *J. Solution Chem.* **44**, 1545 (2015).
8. T. L. Deng, S. Q. Wang, and B. Sun, *J. Chem. Eng. Data* **53**, 411 (2008).
9. D. C. Li, J. S. Yuan, and S. Q. Wang, *Russ. J. Phys. Chem. A* **88**, 42 (2014).
10. D. L. Gao, Y. F. Guo, X. P. Yu, et al., *J. Chem. Eng. Data* **60**, 2594 (2015).
11. F. Li, S. S. Zhang, Y. F. Guo, et al., *Chin. Sci. Paper* **9**, 1080 (2014).
12. S. Q. Wang, X. N. Han, Y. Jing, et al., *J. Chem. Eng. Data* **61**, 1155 (2016).
13. Y. F. Guo, Y. H. Liu, Q. Wang, et al., *J. Chem. Eng. Data* **58**, 2763 (2013).
14. S. Q. Wang, F. Y. Guo, D. C. Li, et al., *Thermochim. Acta* **601**, 75 (2015).
15. J. Gao, Y. F. Guo, S. Q. Wang, et al., *J. Chem.* **2013**, 1 (2013).
16. C. H. Fang, *J. Salt Lake Res.* **2**, 15 (1990).
17. J. M. Speight, *Lange's Handbook of Chemistry*, 16th ed. (McGraw-Hill, New York, 2005).